



Effect of melt temperature on product properties of injection-molded high-density polyethylene

İdris Karagöz¹ · Özlem Tuna²

Received: 27 January 2021 / Revised: 23 March 2021 / Accepted: 7 April 2021 / Published online: 13 April 2021
© The Author(s), under exclusive licence to Springer-Verlag GmbH Germany, part of Springer Nature 2021

Abstract

Recently, injection molding process has generated growing interest, exhibiting great potential to easily fabricate unique polymeric materials for industrial applications. To increase the sustainability of the process, determinative parameters and their effects should be examined. This study focuses on the effect of melt temperature on as-injection molded product, thereby high-density polyethylene samples were fabricated by performing three different melt temperatures (180, 190, and 200 °C), and subsequently, their mechanical, thermal, and morphological and surface quality properties were examined. The results showed that higher melting temperature lowered crystallization rate and decreased the strength of tensile and bending; however, it increased crystal lamellar thickness and impact strength. Moreover, the type of fibrillation changed with the temperature. Moreover, defects formation increased with the temperature. For further application, the effect of the temperature on surface quality was discussed. This work will provide a guide for manufacturing injection-molded products at desired properties by arranging melt temperature.

Keywords Injection molding · Polyethylene · Melting temperature · Warpage · Collapse

Introduction

Injection molding process has been perceived as the most attractive manufacturing technique for plastic materials owing to its numerous advantages in terms of eco-friendliness, easily production with complex geometry and good dimensional accuracy, also suitability for automation [1, 2]. These remarkable advantages make the process a promising manufacturing technique for materials, which can be utilized

✉ İdris Karagöz
idris.karagoz@yalova.edu.tr

¹ Department of Polymer Materials Engineering, Yalova University, 77200 Yalova, Turkey

² Department of Chemical Engineering, Yalova University, 77200 Yalova, Turkey

in both our daily life and commercial sectors such as transportation, construction, electric-electronics, and medical [3, 4]. Despite the fact that structural design, mold design, and technology processing are essential parameters, process conditions, especially temperature, have been significant impact on product quality [1–3, 5, 6]. The molding technology has various temperature concepts such as melt temperature, mold temperature, hydraulic system temperature, granule drying temperature, and outdoor temperature [7, 8].

Melt temperature at which polymer exits the nozzle is known as a determinative parameter for fluidity and flow regime of polymeric material during the molding processing. As the melt temperature is too high, the polymeric material becomes too fluid, thus turbulent flow is observed driven by trapping air and burnt gases in the melt cloud [1, 2, 9]. This behavior can be responsible for sink marks, warpage, shrinkage, and void formation on final material. This problem can be solved with good heat control and reduced cycle time. On the other hand, when this polymer does not melt sufficiently, the mold is not be filled [2, 9]. This situation causes cosmetic defects such as flow marks, weld lines, and poor surfaces, resulting in low product quality. In addition, fragility can be changed by varying the mold temperature. According to the statements, melt temperature has gained research interest to determine its effect on process efficiency and molded plastic product quality. Zhou et al. [2] presented a dynamic method to observe the effect of the melt temperature on polypropylene (PP) material molded with an injection technique. They found that production rate increased at high melt temperature by decreasing the number of cycles to return stability [2]. Mohan et al. [10] also highlighted that melt temperature could change dissolution time and viscosity of the polymer. According to Melo et al. [11], the crystallinity of poly lactic-co-glycolic acid (PLGA) material designed by injection molding process could be controlled with melt processing temperature. This allows the design of implant in desirable geometries with PLGA samples. Zhou and Mallick [12] stated that in case of talc-filled polypropylene, an increase in melt temperature enhanced weld line, resulting cosmetic effect. According to the studies mentioned above, it can be said that the examination of melt temperature is advantageous for high-quality product and highly efficient process.

Studies related to the optimization of process parameters and shortening the cycle time [7, 13, 14], reducing the amount of tension and distortion [10, 11, 14], reduction of unit costs [1, 2], increasing product quality [2, 8, 15], and limiting the number of variables in the process [7, 13] have been conducted by considering materials such as PP [4, 15, 16], polyvinyl chloride (PVC) [8, 17], polystyrene (PS) [8, 9, 12], polyamide 6,6 (PA66), polyoxymethylene (POM) [4, 18], acrylonitrile butadiene styrene (ABS) [5, 8, 19], PC/ABS [18–20], PC [4, 7, 18], polymethylmethacrylate (PMMA) [8, 21], and polybutylene terephthalate (PBT) [8, 20]. Furthermore, the effect of mold surface temperature [22], the measurement of residual stresses [14], and injection pressure [5, 13, 16] have been examined in the injection molding of high-density polyethylene (HDPE) material, which is well-known polymer due to its favorable properties such as easy processability and commercially availability. [23–25].

It can be indicated that no study was conducted on the numerical (measurable-predictable) determination of the effect of melting temperature on material

properties. Although the most common approach is to vary melting temperature to shorten cycle time, increase production rate and eliminate defects such as cosmetic defects encountered in products during the production, it is not clearly known how the properties of as-produced part are affected by rising and lowering the melting temperature. Therefore, this study aims to systematically determine the effect of melting temperature, contributing to eliminate the lack of information on this subject in the literature.

Herein, three different melt temperatures were carried out to examine the properties of the as-obtained high-density polyethylene (HDPE) and the examination was driven by characterization methods, namely scanning electron microscopy (SEM), differential scanning calorimetry (DSC), tensile and flexural test, impact test, hardness measurement, and surface quality measurement (surface gloss and surface roughness). In addition, the amount of collapse and distortion was measured by performing a new method based on visual imaging solution.

Materials and methods

Materials

High-density polyethylene (HDPE) was supplied by PETKIM and the polymer is coded as PETILEN YY S 0464. Stabilizer (Ciba Irgafos® 168) was purchased from Ciba Specialty Chemicals LTD. All the materials were used without any purification. The typical properties of the polyethylene in the form of compression-molded sheet, which were obtained from Technical Data Sheet of PETILEN YY S 0464, were considered as reference values and the related values are presented in Table 1. Also, the values were checked with characterization methods mentioned below for injection-molded HDPE product.

Table 1 Typical properties of PETILEN YY S 0464 [26]

Properties	Condition	Method	Unit	General purpose
Melt flow rate	190 °C, 2.16 kg	ASTM D1238	g/10 min	0.36
Density	23 °C	ASTM D1505	g/cm ³	0.961
Tensile strength	23 °C	ASTM D638	MPa	30
Tensile modulus	23 °C	ASTM D638	MPa	1200
Flexural strength	23 °C	TS EN ISO 178	MPa	27.50
Flexural modulus	23 °C	TS EN ISO 178	MPa	1100
Izod impact strength	23 °C	ASTM D256	kJ/m ²	66
Hardness	23 °C	ASTM D2240	Shore D	65
Vicat softening point	10 °C/min	ASTM D1525	°C	128
Melting point (DSC)	50 N, 120 °C/h	ASTM D3417	°C	134.1

Injection molding process

The injection molding process was performed using an Engel Victory injection molding machine (Model 80) with the force of 800 kN. The HDPE samples were pre-dried in an oven at 40 °C for 3 h to remove the surface moisture. The materials were fed into the molding machine and subsequently injected into the molds, whose dimensions were determined based on ISO 527 and ISO 180 for tensile test and impact test, respectively. In this molding, injection speed, injection pressure, back pressure, screw speed, and cushion/pad were determined as 65 mm/s, 80 bar, 3 bar, 150 rpm, and 6.35 mm, respectively. Different melting behaviors were observed by applying three different nozzle temperatures (180, 190, 200 °C), as the nozzle temperature is determinative for the degree of melting which is attributed to the flow rate of the melt, indicating that the temperature plays crucial role on the degree of filling the polymer into the mold, resulting in the mechanical properties of final molded product. On the other hand, taking into account the lower and upper limits of the process temperature of the material, the nozzle temperature should be changed between 10 and 20 °C (without changing the temperatures of other regions). Thus, a study was designed so that the difference between nozzle temperature values increased by 10 °C. In addition, the other temperature parameters are depicted in Table 2.

Characterization

Tensile and flexural properties were measured using a Zwick Z020 Model testing machine with a 20 kN load cell. The tensile test was conducted according to ASTM D638, and the test was performed at room temperature and at a drawing rate of 50 mm/min. According to the draw rate, it can be calculated that the corresponding engineering strain rates were $2 \times 10^{-3} \text{ s}^{-1}$. The bending test was performed based on TS EN ISO 178, and the test was performed at room temperature and at a bending rate of 2 mm/min. An izod impact test was performed using a Zwick Roel Model tester (with a 5.5 J hammer) according to ASTM D256. All the strength measurements were performed in quintuple. A hardness test was conducted in a Zwick Roel device according to the ASTM D2240 standard by using a Shore D scale. The morphology of fractured surfaces of the materials from the impact test was investigated using an Inspect S50 Model electron microscopy (SEM). The samples were coated

Table 2 Injection molding parameters

Sample Code	Processing temperatures (°C)					
	Rear zone	Center zone	Front zone	Nozzle	Melt	Mold
N180	160	170	180	180	180	50 ± 5
N190	160	170	180	190	190	50 ± 5
N200	160	170	180	200	200	50 ± 5

with 100 Å gold under vacuum to obtain an inert and permeable surface, and the microstructures were photographed under 20 kV voltage.

Thermal properties were examined using a differential scanning calorimetry (DSC, Seiko DSC 7020 Model). The relevant test was applied based on ASTM D3417. DSC analyses were performed under nitrogen atmosphere to observe the thermal transitions and crystallization degree of the as-obtained materials. The crystallinity is considered by using the equation as follows:

$$X_c = \frac{\Delta H_m}{\Delta H^{\circ}_m} \times 100 \quad (1)$$

where ΔH_m represents the melting enthalpy and ΔH°_m refers to 100% crystalline enthalpy value of HDPE (293 J/g) [27, 28].

Linear polymers such as HDPE are known to crystallize from their melt into regular lamellar structures when cooled below their melting point. According to the behavior of the linear polymers, the required melting enthalpy value (ΔH_m) was determined by considering isothermally crystallized samples. Therefore, to determine the degree of crystallinity (X_c) of the as-molded HDPE samples in this study, the melting curves of cold crystallized HDPE samples were recorded by applying DSC measurement. Firstly, temperature scale of the DSC was calibrated from the melting point of high-purity (99.999%) metals: tin (231.93 °C) and indium (156.60 °C). The power response of the calorimeter was calibrated from the enthalpy of fusion of indium. Secondly, samples were weighed accurately using a microbalance to 10 µg. About 15.0 mg was used encapsulated in an aluminum pan, and an empty aluminum pan was used as reference. Then, the isothermally crystallized samples were prepared as follows: The samples were heated to 210 °C at a heating rate of 50 °C/min and maintained at 210 °C for 5 min, then the samples were cooled down to 80 °C at a cooling rate of 10 °C/min. After the isothermal crystallization, the samples were heated immediately to 190 °C at 10 °C/min heating rate to obtain melt samples. Then, the second heating curves were obtained. Finally, the curves were used to calculate the degree of crystallinity (X_c (%)) of the samples.

In addition, the Gibbs-Thomson equation allows for the prediction of the melting point as a function of the lamellar thickness. The relevant equation was shown as follows:

$$\frac{T_m}{T^{\circ}_m} = 1 - \frac{2\delta e}{\Delta H_m} \quad (2)$$

where T_m represents the melt temperature, T°_m refers to equilibrium melt temperature of HDPE (146 °C), and free surface energy of crystals (δe) was used as 90 mJ/m² [27]. In addition, Vicat softening temperature (VST) was measured by using an Instron Ceast HV3 Model machine according to ASTM D1525. A load of 50 N was applied to the specimens. The specimens were then lowered into an oil bath at 23 °C. The bath was raised at a rate of 120 °C per hour until the needle penetrates 1 mm.

Investigation of warpage and collapse formation

The formation of warpage and collapse was determined using a video measuring system on SmartScope ZIP Advance 250 Model (OGP Company) and a comparator with an accuracy of ± 0.001 , whose brand is Mitutoya. The related device consists of a digital camera and a high-precision lens. The depth of the warpage was indicated by auto-focus feature in Z axis and the amount of collapse was calculated by defining the measurements from different points. Tension and distortion measurements were performed using an ISO 527-2 1A type tensile test rod with 4 mm thickness and 75 mm inter-jaw distance. The samples placed on a flat base on the device were scanned in 3D on the SmartScope ZIP Advance 250 Model device using a Vu-Light LED illuminator at a distance of 38 mm and laser support over the lens. After scanning, the tensions and distortions on the x , y , and z axes were determined using the MeasureMind 3-D® MultiSensor metrology software. In the measurements performed with a comparator, the tensile test rod was fixed on a cast plate. The linear dimensions of the test specimen were scanned with the comparator along a line determined from the midpoint. The dimensions between the measurement start and end points, and the deviations in thickness were measured. The data obtained from the MeasureMind 3-D® MultiSensor metrology software were compared with the comparator measurement results and observed to be compatible.

Surface quality measurement

The surface quality was indicated with respect to surface roughness and surface gloss measurements. Surface roughness measurements were performed in accordance with the ISO Class 3 in a Mitech MR200 (Onalxon) surface roughness measuring device with a Rz measurement range of 0.1–50 μm , by using 1.0 mm/s feed rate, 0.4 mN load, and a diamond detector tip with a diameter of 5 μm . Surface gloss measurements were performed in an Elcometer micro-gloss device at a 60° projection angle.

Table 3 Mechanical test results of the materials

Sample code	Tensile strength (MPa)*	Tensile modulus (MPa)*	Flexural strength (MPa)*	Flexural modulus (MPa)*
Reference	30.00 \pm 0.00 ⁻	1200 \pm 00 ⁻	27.50 \pm 0.00 ⁻	1100 \pm 00 ⁻
N180	28.19 \pm 0.11 ^b	1105 \pm 67 ^c	23.74 \pm 0.05 ^a	1225 \pm 35 ^b
N190	26.20 \pm 0.17 ^b	1050 \pm 47 ^b	25.04 \pm 0.07 ^a	1360 \pm 23 ^a
N200	27.84 \pm 0.09 ^a	1120 \pm 33 ^b	24.35 \pm 0.23 ^c	1220 \pm 35 ^b

*Mean values followed by similar letters in the column do not show statistical ($p \geq 0.05$)

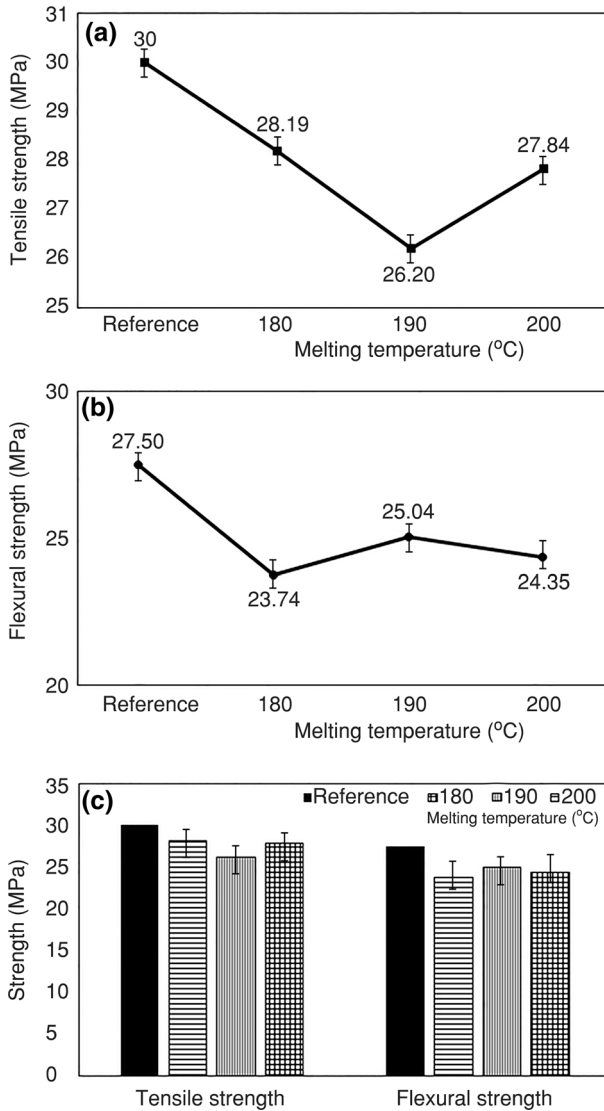


Fig. 1 Result of tensile and flexural test, **a** Tensile strength, **b** Flexural strength, **c** Comparison of the tensile and flexural strength

Results and discussion

Mechanical properties

Tensile, bending, and impact strengths are main mechanical parameters for polymeric materials to determine application area and time. The tensile and flexural properties of the as-fabricated HDPE samples with injection molding at different

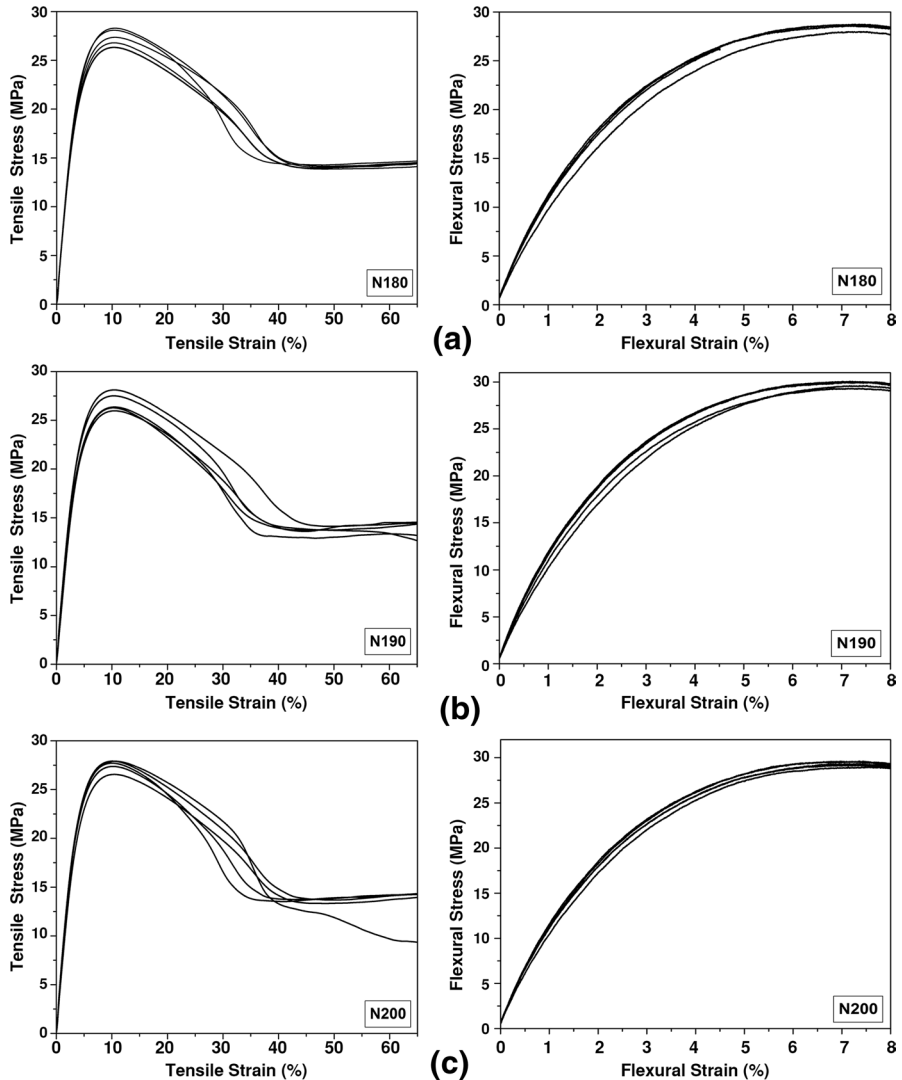


Fig. 2 Result of tensile and flexural stress–strain curves, **a** N180, **b** N190, **c** N200

melt temperatures are presented in Table 3 and Fig. 1. Furthermore, tensile and bending stress–strain curves are presented in Fig. 2. The tensile strength decreased first and then increased in temperature range from 180 to 200 °C. According to previous studies, short fibers caused decreasing the strength of the polymeric material [29]. Furthermore, it was presented that high melting temperature resulted in the formation of inequality crystals on surface, which was attributed to decrease the tensile properties [30]. On the other hand, the increment provided more effective crystallization ratio, resulting in higher durable material [11]. The other indication was that high melt temperature decreased the flow resistance (viscosity) of polymer

melt, so the mold was properly filled with the polymer melt and the final molded product showed improved yield stress [31]. Therefore, it can be indicated that in this study, when the temperature increased from 180 to 190 °C, the shortage of fiber length and the direction of crystallization decreased the tensile strength. In further temperature increase, the crystallization ratio and the length of polymer chains were enhanced, so the tensile property increased. The changes in fiber structure and crystallization ratio were supported with SEM and DSC results. Regarding the result of the reference value (30 MPa), it can be also said that the melt temperature of 180 °C was enough to obtain the expected strength. This shows that the HDPE solid crystal was in the equilibrium with the molten polymer at the temperature and the cooling time was sufficient to get ordered structure, resulting in higher tensile strength [1, 31]. In addition, it can be stated that for the melting temperatures, the process variability was quite low due to the strength values with their respective low standard deviations. Notably, the standard deviation of N200 was lower as compared to N180 and N190, indicating that more consistent results at the highest melting temperature. Likewise, the bending test results were more logical in terms of N180.

In terms of flexural properties, it can be indicated that the three melt temperatures did not cause the material to lose its flexibility, since the breakage did not observe during the bending test. As seen in Fig. 1 and Table 3, the values of bending strengths were recorded when 5% stretching occurred. Depending on the melt temperature, the bending strengths increased first and then decreased. The increase

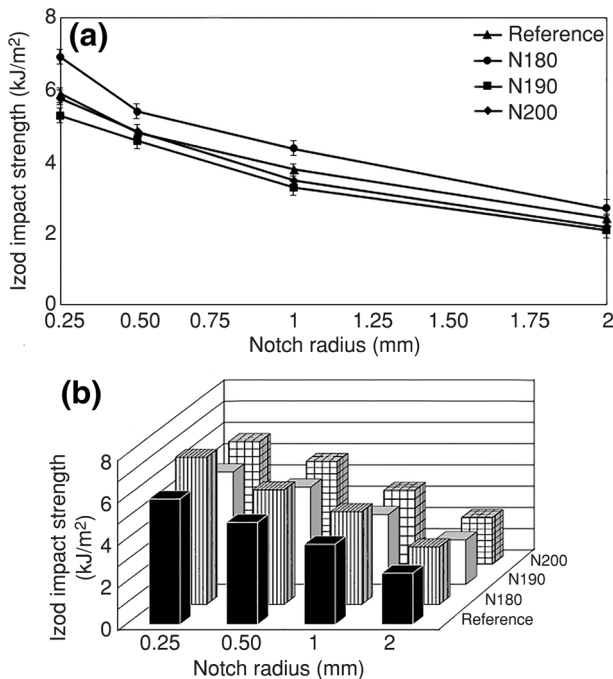


Fig. 3 Results of impact test, **a** effect of notch radius on impact strength, **b** comparison of result of impact test

could be due to higher crystallization ratio at 190 °C than that of 180 °C. Moreover, the decrease at the final temperature could be driven by residual stresses due to the difference in molecular mobility with respect to melt temperature during cooling [19, 20]. In addition, the bending strength value obtained at 190 °C was closest to the value of the reference. It can be therefore stated that the as-prepared HDPE material could show more desirable resistance through bending at 190 °C.

The izod impact strengths were also examined for mechanical properties of the products in Fig. 3. The resistance of impact decreased with increasing temperature and notch radius. The reason for the result could be residual stresses and crystallization ratio. The property could be arranged with only changing process parameters, such as holding pressure and cycle time [7, 32, 33]. This gives an opportunity to fabricate high-quality and high-strength products in an easy way [3, 21, 31].

In addition, the measurement of hardness was performed with respect to melt temperature. The value was found to 66, 65, and 64 Shore D at 180, 190, and 200 °C, respectively, as well as the reference hardness value was 65 Shore D. That is to say, there was no remarkable change on the hardness property depending on melt temperature. The increase in melt temperature limited the thickening of the solidified surface due to rapid cooling [34]. It can be therefore stated that the thickness of the mold surface was in similar value with the upper surface of the HDPE product between 180 and 200 °C of melt temperature. On the other hand, it can be predicted that the hardness value differed the material surface to the inner parts depending on solidification rate [27, 32, 35].

Thermal properties

The exclusive formation of crystals plays a significant role in the quality of the molded product. Herein, to confirm the effect of melt temperature on thermal properties, the crystallization ratio and crystal lamella thicknesses were examined by DSC. The melting point was found to be 135.6 °C, 136.9 °C, and 135.9 °C at N180, N190, and N200 °C, respectively, as well as the reference melting point was 134.1 °C. The representative DSC thermograms of the samples after injection molding and the relevant values related to the crystallization behavior are shown in Fig. 4. In Fig. 4a, a significant change was not observed at different melt temperatures, while the crystal melting temperature (T_m) of the as-molded samples was measured 1.5–2.8 °C higher than that of the reference value. This could be due to the mostly linear structure of HDPE at similar line with the study performed by Jiang et al. [36]. It can be estimated that no branching occurred in the polymer chain due to the changes in the melt temperature. As depicted in Fig. 4b, at all melt temperatures, the crystallization ratio increased as compared to the reference value. The difference could result from the solidification kinetics, spheroid size, and microstructure formed regarding the melt temperature [35, 37–40]. It is likely that 180 and 200 °C of the melt temperature promoted crystallization ratio with similar number of crystals, however, the movement and the rearrangement of molecular chains of HDPE could be retarded during the solidification process and the crystallinity was reduced [41]. The behavior agrees with the results of mechanical tests.

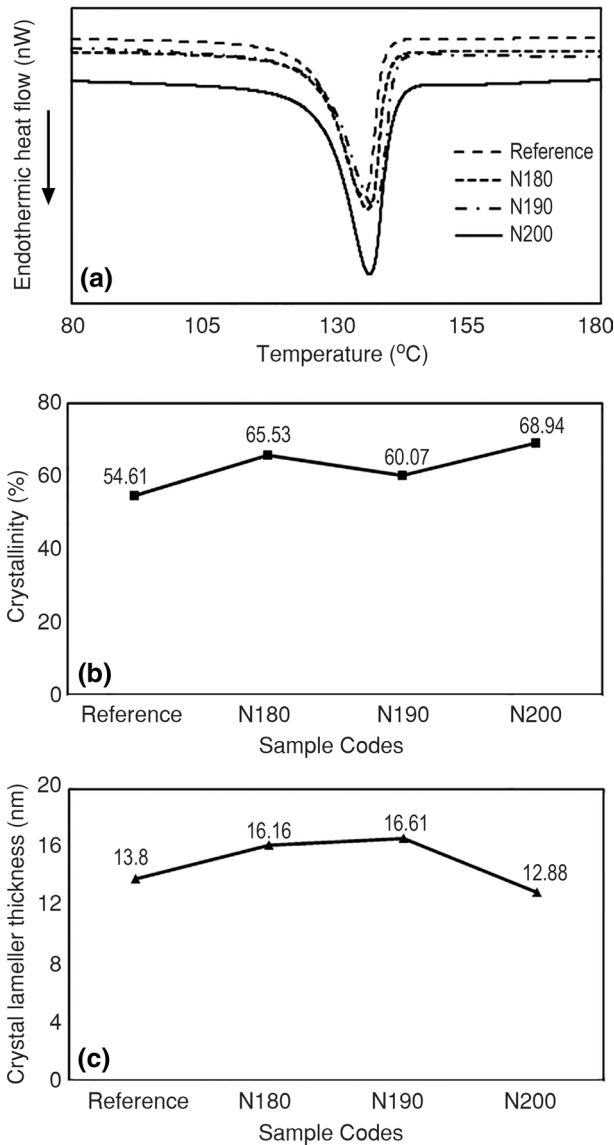


Fig. 4 Results of DSC test **a** DSC curves, **b** comparison of crystallization percentages and crystal lamellar thickness

The crystal lamella thicknesses are presented in Fig. 4c. When the results were examined, it is indicated that the thickness decreased with the amount of crystallization. Similar result was observed in the literature [16, 40–43]. The possible different cooling behavior at 200 °C could cause the enhancement of the thickness [44]. It is therefore stated that the melt temperature is effective parameter on the rate of crystallization and lamella thicknesses in terms of injection molding of HDPE.

In addition, vicat softening temperature was measured to evaluate the heat resistance of the injection-molded HDPE products. The temperature was around 128 °C for the reference value. The values of the as-molded products were enhanced with the melt temperature. Vicat softening temperature was found to be 129.2 °C, 129.7 °C, 128.6 °C for N180, N190, and N200, respectively. Notably, 190 °C should be applied as melt temperature in the injection molding of HDPE to achieve better heat resistance. The statement could be due to the crystallization kinetics and the crystal lamella thicknesses at 180 and 200 °C as compared 190 °C [16, 38].

Morphological properties

In order to determine the microstructure of the as-obtained samples, SEM micrographs are presented in Fig. 5. The morphology analyses exhibit that the melt temperature changed the morphology of the products at similar line with studies [9, 29, 31]. The different cooling behavior driven by varying melting temperatures could change the amount of volumetric shrinkage [17, 35, 40]. In this study, the density of

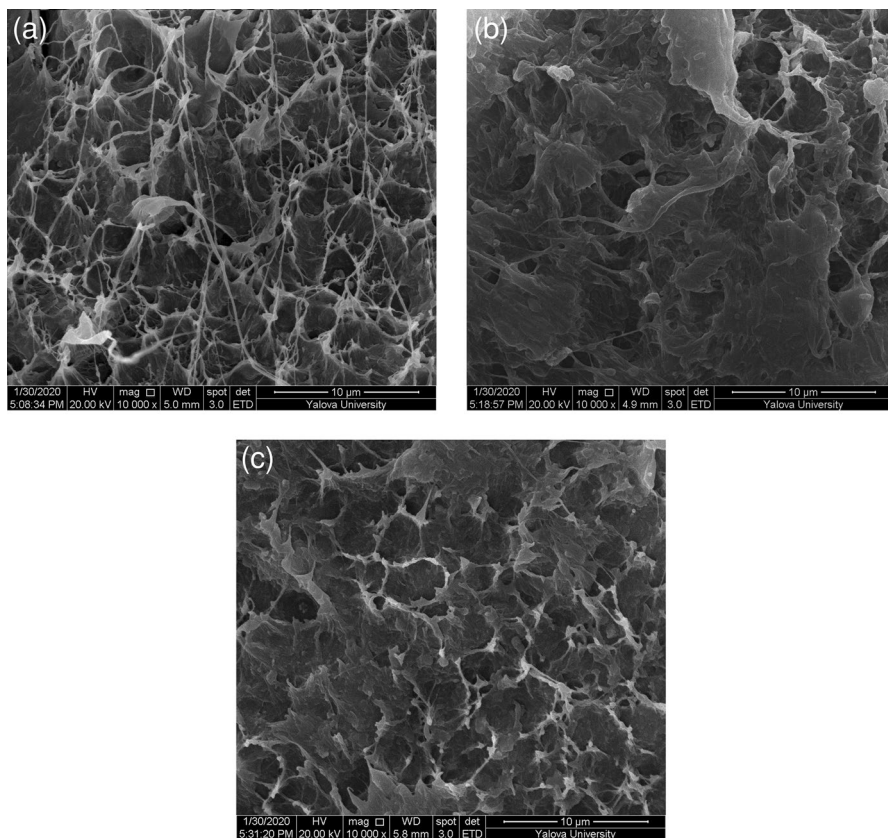


Fig. 5 SEM photographs **a** N180, **b** N190, **c** N200

fibrils and the length of fibrils decreased with melt temperature, resulting in a hollow lattice. Similar result was obtained by some research [33, 45–47]. As known, lower density fibrillation and long fibrils increased the flexibility, while shortness and hollow lattice decreased it. Moreover, the formation of hollow could change depending on volumetric expansion and cooling behavior driven by crystallization behavior and melting temperature [30, 33, 48]. That is to say, the morphological structure affected the mechanical and the thermal properties of the molded product [16, 33]. Herein, the statement could be supported with the impact test and DSC results. Although the hollow into the structure of the as-molded product presented a disadvantage for mechanical properties [16], to obtain high-quality micro-nano-structure, it was required [38]. Kong et al. [49] showed that cavity formation, crystallization ratio, and spherulite size could change with the usage of fillers, additives, and nucleating agents, resulting in the control of the morphology. It can be therefore said that the melt temperature should be considered to fabricate promising product with desired properties such as nano-structure and high-crystallization ratio.

An effect similar to that of the melting temperature on the microstructure was observed in a previous study examining the mold surface temperature [22]. Temperatures, such as mold surface temperature, melting temperature, and hydraulic system temperature, affect the microstructure. When the mold surface temperature was increased by +10 °C, fibrillation increased, while the fibril lengths were reduced [22]. Unlike the effect of mold surface temperature, the increase in melting temperature by +10 °C significantly reduced fibrillation. When the temperatures reached the upper limit values recommended for the process, similar observation was obtained for both different temperature process parameters.

Warpage and collapse formation

The most significant defects of polymer part are warpage and collapse are in terms of quality in the process of injection molding. The results of the measurement, the images related to collapse in the direction of x axis, and the mapping of the warpage in the part based on the direction are presented in Table 4, Fig. 6, and Fig. 7, respectively. The differences in color driven by the amount of collapse (Fig. 6) were compatible with the measurement values (Table 4). In case of 180 °C melt temperature, the highest warpage and collapse formation was observed in dimensionally larger parts. At 190 °C, the relevant defect ratio also increased at the thin part cross section and the long edges of the sample, which

Table 4 Collapse and warpage of the materials

Sample code	Collapse (%)	Warpage (%)	Warpage rates according to axes (mm)		
			x	y	z
N180	+5	+2	+0.033	+0.028	+0.029
N190	+6	+5	+0.037	+0.026	+0.025
N200	+7	+8	+0.139	+0.128	+0.129

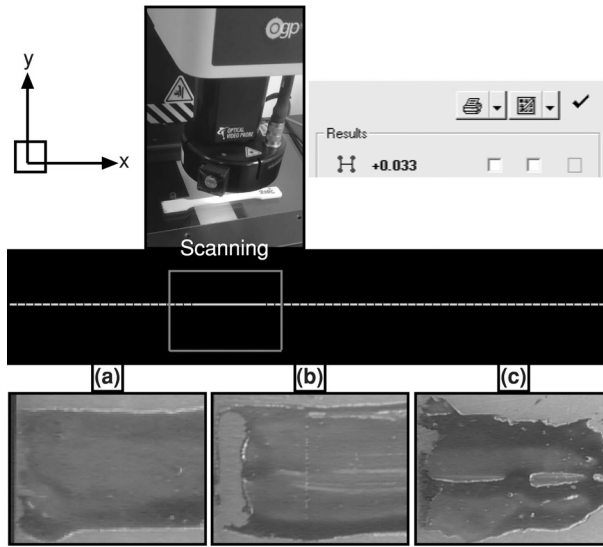


Fig. 6 Warpage and collapse formation measurement photographs **a** N180, **b** N190, **c** N200

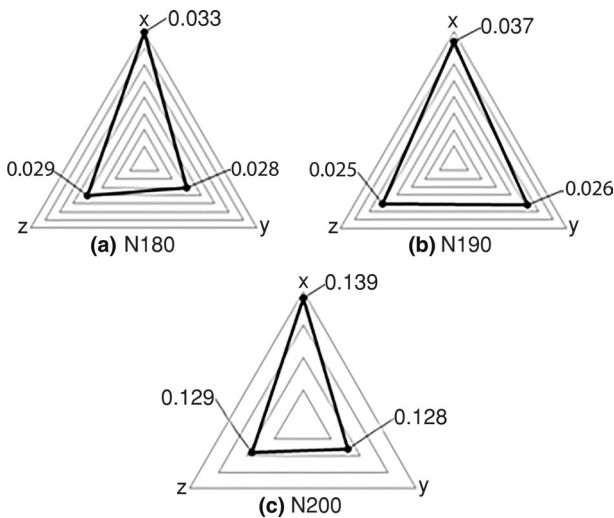


Fig. 7 Mapping of the amount of warpage according to axes **a** N180, **b** N190, **c** N200

are attributed to collapse and warpage formation, respectively. In addition, both defect types occurred on all surfaces of the as-molded part depending on wall thickness at the melt temperature of 200 °C. Overall trend is that the increase in the melt temperature enhanced the amount of warpage and collapse formation, especially thin parts of the sample. The similar result was observed in the literature [5, 30, 32]. The behavior can be due to the cooling difference caused by the rapid solidification of the outer part, which contacts with the mold surface

and subsequently the continuation of solidification toward the inner regions. In case of higher melt temperature, the warpage formation increases because of the mobility in molecule chains and the tendency to rearrange the structure, resulting from longer cooling time [5]. To conclude, the melt temperature has significant effect on the amount of warpage and collapse formation on the injection-molded HDPE material and the importance of the effect changes depending on the thickness of the part, resulting in the design of the part. That is to say, the melt temperature should be adjusted in a correct way to improve process efficiency and product quality [3, 21].

Surface quality

The quality of plastic products manufactured by injection molding process is highly influenced by the properties of as-molded surfaces, which are assigned to surface gloss and surface roughness. Herein, both properties were implemented, and the results obtained by the measurements are presented in Table 5. Considering the physical pre-control on the quality of the parts, burr formation was examined based on melt temperature. It was observed that flash burr formation in the parts increased with melt temperature. This can be due to the material overflowing to the mold joining surface. In terms of surface gloss measurement, the surface gloss class obtained at 200 °C and 190 °C was determined to be semi-gloss and the surface gloss class at 180 °C to be satin-like finish. This situation can be due to change in the material fluidity at different melt temperatures [42]. Surface roughness, which is expressed as the irregularities of material resulted from various process conditions, increased with melt temperature in this study. This can be driven by the heat transfer rate between the mold and the melt. A frozen polymer layer is formed between the polymer melt and the mold surface. This non-melt polymer layer does not allow the molten polymer to penetrate the voids on the surface [34]. Lui and Gehde [30] were also observed this result. Therefore, it can be stated that differences in melt temperature significantly affected the surface quality of as-molded HDPE parts at line with Berger et al. [42].

Table 5 Surface roughness and surface gloss improved efficiency under different mold surface temperature

Sample code	Melting temperature (°C)	Surface roughness (Rz, μm)	Roughness improved. efficiency (%)	Surface gloss (GU 60°)	Gloss improved. efficiency (%)
N180	180	20.0	–	30–34	–
N190	190	17.6	+ 12	35–40	+ 17
N200	200	11.8	+ 58	55–60	+ 80

Conclusion

In this study, HDPE samples were successfully molded by injection method under different melt temperature. The characteristics of the samples were investigated to clarify the effect of the melt temperature on product quality. The significant results are presented as follows:

1. Higher melt temperature has potential to improve rate of crystallization and impact strength, while this situation causes a decrease in the resistance against tensile and bending strengths. In a previous study examining the effect of mold surface temperature [22], it was observed that the tensile and bending strength increased and the impact strength decreased as the mold surface temperature increased. It can be indicated that the melting temperature is an important parameter in applications in which impact strength is important, while the mold surface temperature is an important parameter in applications in which tensile and bending strength is important.
2. The characterization part related to the measurement of impact strength indicates that the notch effect (different notch diameters) should be considered as an additional parameter to determine injection molding efficiency. The linear decrease in the values obtained in the tests of the samples with different notch diameters may indicate that the production continues under optimum conditions and that the number of defective products will decrease.
3. It is shown that the melt temperature plays role in crystal melting temperature, suggesting that the melt temperature should definitely be taken into consideration for products utilized under thermal load.
4. In terms of microstructure, the increase in the melt temperature results in higher void formation and lower fibrillation rate in the structure depending on expansion and cooling times of the HDPE sample during the molding process. Moreover, it can be said that lower fibril density and long fibril length increase the flexibility of the materials, while the property reduces by larger amount of hollow in the structure. Similar results were observed by examining the effect of mold temperature in the previous study [22]. It can be indicated that in the process, higher temperature profiles promote the formation of microstructures, whereas lower temperature range inhibits fibril and void formation.
5. An increase in melting temperature of + 10 °C increases the amount of collapse by around 1% and it enhances the warpage amount by approximately 3%, resulting that the melt temperature is an important parameter for the formation of defects during the injection molding of HDPE. Also, the mold surface temperature affected the amount of slump and distortion in a similar way.
6. Surface quality can change by the melt temperature: It improves the surface brightness and the surface roughness, indicating that the melt temperature is critical parameter for products in which surface brightness is important. On the other hand, higher molding temperature decreases the brightness

7. The study shows that the melting temperature is a remarkable effective process variable when other process parameters are kept constant. The effectiveness can be limited when more than one process variable is examined.

Acknowledgements The authors gratefully acknowledge the financial support (Project No: 2020/F/0001) of Yalova University Scientific Research Projects Coordination Unit.

References

1. Katmer Ş, Karatas Ç (2012) The effects of molding conditions on the residual stresses in injection molded polystyrene flat parts. *J Fac Eng Archit Gazi Üniv* 27(3):501–507
2. Zhou X, Zhang Y, Mao T, Zhou H (2017) Monitoring and dynamic control of quality stability for injection molding process. *J Mater Process Technol* 249:358–366. <https://doi.org/10.1016/j.jmatpotec.2017.05.038>
3. Kurt M, Kaynak Y, Kamber ÖS, Mutlu B, Bakır B, Koklu U (2010) Influence of molding conditions on the shrinkage and roundness of injection molded parts. *Int J Adv Manuf Technol* 46:571–578. <https://doi.org/10.1016/j.jmatprotec.2017.05.038>
4. Meister S, Drummer D (2013) Investigation on the achievable flow length in injection moulding of polymeric materials with dynamic mould tempering. *Sci World J*. <https://doi.org/10.1155/2013/845916>
5. Chang TC, Faison E (2001) Shrinkage behavior and optimization of injection molded parts studied by the taguchi method. *Polym Eng Sci* 41(5):703–710. <https://doi.org/10.1002/pen.10766>
6. Brooks NW, Duckett RA, Ward IM (1992) Investigation into double yield points in polyethylene. *Polymer* 33(9):1872–1880. [https://doi.org/10.1016/0032-3861\(92\)90486-G](https://doi.org/10.1016/0032-3861(92)90486-G)
7. Xu Y, Zhang Q, Zhang W, Zhang P (2015) Optimization of injection molding process parameters to improve the mechanical performance of polymer product against impact. *Int J Adv Manuf Technol* 76:2199–2208. <https://doi.org/10.1007/s00170-014-6434-y>
8. Singh G, Verma A (2017) a brief review on injection moulding manufacturing process. *Mater Today Proc* 4:1423–1433. <https://doi.org/10.1016/j.matpr.2017.01.164>
9. Zhang L, Zhao G, Wang G (2017) Formation mechanism of porous structure in plastic parts injected by microcellular injection molding technology with variable mold temperature. *Appl Therm Eng* 114:484–497
10. Mohan M, Ansari M, Shanks RA (2017) Review on the effects of process parameters on strength, shrinkage, and warpage of injection molding plastic component. *Polym Plast Technol Eng* 56(1):1–12. <https://doi.org/10.1080/03602559.2015.1132466>
11. de Melo LP, Salmoria GV, Fancello EA, Roesler CRdM (2017) Effect of injection molding melt temperatures on PLGA craniofacial plate properties during in vitro degradation. *Int J Biomater*. <https://doi.org/10.1155/2017/1256537>
12. Zhou Y, Mallick PK (2005) Fatigue performance of an injection molded talc-filled polypropylene. *Polym Eng Sci* 45(4):510–516. <https://doi.org/10.1002/pen.20284>
13. Mao Q, Wyatt TP, Chen J, Wang J (2015) Insert injection molding of high-density polyethylene single-polymer composites. *Polym Eng Sci* 55(11):2448–2456. <https://doi.org/10.1002/pen.24132>
14. Moayyedean M, Abhary K, Marian R (2018) Optimizing of injection molding process based on fuzzy quality evaluation and taguchi experimental design. *J Manuf Sci Technol* 21:150–160. <https://doi.org/10.1016/j.cirpj.2017.12.001>
15. Dang XP (2014) General frameworks for optimization of plastic injection molding process parameters. *Simul Model Pract Theory* 41:15–27
16. Katmer Ş, Karataş Ç (2015) Effects of injection molding conditions on residual stress in HDPE and PP parts. *J Fac Eng Archit Gazi Üniv* 30(3):319–327. <https://doi.org/10.17341/gummfd.45855>
17. Rathi MG, Salunke MD (2012) Analysis of injection moulding process parameters. *Int J Eng Res Technol* 1(8):1–5

18. Erzurumlu T, Ozcelik B (2006) Minimization of warpage and sink index in injection-molded thermoplastic parts using taguchi optimization method. *Mater Des* 27:853–861. <https://doi.org/10.1016/j.matdes.2005.03.017>
19. Somé SC, Delaunay D, Faraj J, Bailleul JL, Boyard N, Quilliet S (2015) Modeling of the thermal contact resistance time evolution at polymer-mold interface during injection molding: effect of polymers' solidification. *Appl Therm Eng* 84:150–157. <https://doi.org/10.1016/j.applthermaleng.2015.03.037>
20. Nian SC, Wu CY, Huang MS (2015) Warpage control of thin-walled injection molding using local mold temperatures. *Int Commun Heat Mass Transf* 61:102–110. <https://doi.org/10.1016/j.ichea.2014.12.008>
21. Tsai KM, Lan JK (2015) Correlation between runner pressure and cavity pressure within injection mold. *Int J Adv Manuf Technol* 79:273–284. <https://doi.org/10.1007/s00170-014-6776-5>
22. Karagöz İ (2020) An effect of mold surface temperature on final product properties in the injection molding of high-density polyethylene materials. *Polym Bull*. <https://doi.org/10.1007/s00289-020-03231-2>
23. Jordan JL, Casem DT, Bradley JM, Dwivedi AK, Brown EN, Jordan CW (2016) Mechanical properties of low density polyethylene. *J Dyn Behav Mater* 2(4):411–420. <https://doi.org/10.1007/s40870-016-0076-0>
24. Furmanski J, Cady CM, Brown EN (2013) Time-temperature equivalence and adiabatic heating at large strains in high density polyethylene and ultrahigh molecular weight polyethylene. *Polymer* 54(1):381–390. <https://doi.org/10.1016/j.polymer.2012.11.010>
25. Brown EN, Willms RB, Gray GT, Rae PJ, Cady CM, Vecchio KS, Flowers J, Martinez MY (2007) Influence of molecular conformation on the constitutive response of polyethylene: a comparison of HDPE, UHMWPE, and PEX. *Exp Mech* 47(3):381–393. <https://doi.org/10.1007/s11340-007-9045-9>
26. Petkim Product Specifications Catalogue (2020) PETILEN YY S 0464 high density polyethylene (HDPE) technical data sheet. <https://www.petkim.com.tr/Sayfa/2/1780/TECHNICAL-DATA-SHEETS-AND-PRODUCT-SPECIFICATIONS.aspx>. Accessed 10 May 2020
27. Karagöz İ, Öksüz M (2018) Microstructures occurring in the joined thermoplastics sheets with friction stir welding. *J Fac Eng Archit Gazi Üniv* 33(2):503–515. <https://doi.org/10.17341/gazimmfd.416359>
28. Manzur A (2008) Strain rate effect on crystallinity variations in the double yield region of polyethylene. *J Appl Polym Sci* 108(3):1574–1581. <https://doi.org/10.1002/app.27806>
29. Feldmann M (2016) The effects of the injection moulding temperature on the mechanical properties and morphology of polypropylene man-made cellulose fibre composites. *Compos A* 87:146–152. <https://doi.org/10.1016/j.compositesa.2016.04.022>
30. Liu Y, Gehde M (2016) Effects of surface roughness and processing parameters on heat transfer coefficient between polymer and cavity wall during injection molding. *Int J Adv Manuf Technol* 84:1325–1333. <https://doi.org/10.1007/s00170-015-7816-5>
31. Dar UA, Xu YJ, Zakir SM, Saeed MU (2017) The effect of injection molding process parameters on mechanical and fracture behavior of polycarbonate polymer. *J Appl Polym Sci* 134(7):1–9. <https://doi.org/10.1002/app.44474>
32. Banik K (2008) Effect of mold temperature on short and long-term mechanical properties of PBT. *Express Polym Lett* 2(2):111–117. <https://doi.org/10.3144/expresspolymlett.2008.15>
33. Chen SC, Yang JP, Hwang JS, Chung MH (2008) Effects of process conditions on the mechanical properties of microcellular injection molded polycarbonate parts. *J Reinf Plast Compos* 27(2):153–165. <https://doi.org/10.1177/0731684407082542>
34. Maghsoudi K, Jafari R, Momen G, Farzaneh M (2017) Micro-nanostructured polymer surfaces using injection molding: a review. *Mater Today Commun* 13:126–143. <https://doi.org/10.1016/j.mtcomm.2017.09.013>
35. Yang B, Ding MY, Hu L, Li GJ, Miao JB, Gao X, Li XB, Zhang B, Su LF, Chen P, Qian JS (2019) Melt crystallization behavior of injection-molded high-density polyethylene based upon a solidification kinetic analysis. *J Macromol Sci Part B Phys* 58(1):42–58. <https://doi.org/10.1080/00222348.2018.1476429>
36. Jiang L, An M, Wu F, Miao W, Wang Z, Zhang Y, Hsiao BS (2018) The influence of short chain branch on formation of shear induced crystals in bimodal polyethylene at high shear temperatures. *Eur Polym J* 105:359–369. <https://doi.org/10.1016/j.eurpolymj.2018.03.036>

37. Chalid M, Fikri AI, Satrio HH, Joshua M, Fatriansyah JF (2017) An investigation of the melting temperature effect on the rate of solidification in polymer using a modified phase field model. *Int J Technol* 7:1321–1328. <https://doi.org/10.14716/ijtech.v8i7.707>
38. Fischer E (1972) Effects of annealing and temperature on the morphological structure of polymers. *Pure Appl Chem* 31(1–2):113–132. <https://doi.org/10.1351/pac197231010113>
39. Iyer K, Margossian M, Muthukumar M (2019) Interlude of metastability in the melting of polymer crystals. *J Chem Phys*. <https://doi.org/10.1063/1.5114645>
40. Mohammadi H, Vincent M, Marand H (2018) Investigation the equilibrium melting temperature of linear polyethylene using the non-linear hoffman-weeks approach. *Polymer* 46:344–360. <https://doi.org/10.1016/j.polymer.2018.05.049>
41. Kuzmanović M, Delva L, Cardon L, Ragaert K (2016) The effect of injection molding temperature on the morphology and mechanical properties of PP/PET blends and microfibrillar composites. *Polymers*. <https://doi.org/10.3390/polym8100355>
42. Berger GR, Pacher GA, Pichler A, Friesenbichler W, Gruber DP (2014) Influence of mold surface temperature on polymer part warpage in rapid heat cycle molding. *AIP Conf Proc*. <https://doi.org/10.1063/1.4873761>
43. Kazmierczak T, Galeski A, Argon AS (2005) Plastic deformation of polyethylene crystals as a function of crystal thickness and compression rate. *Polymer* 46(21):8926–8936. <https://doi.org/10.1016/j.polymer.2005.06.073>
44. Rastogi S, Spoelstra A, Gossens J, Kemstra P (1997) Chain mobility in polymer systems: on the borderline between solid and melt. 1. Lamellar doubling during annealing of polyethylene. *Macromolecules* 30(25):7880–7889. <https://doi.org/10.1021/ma970519o>
45. Prud'homme RE, (2016) Crystallization and Morphology of Ultrathin Films of Homopolymers and Polymer Blends. *Prog Polym Sci* 54:214–231. <https://doi.org/10.1016/j.progpolymsci.2015.11.001>
46. Brener E, Müller-Krumbhaar H, Temkin D (1996) Structure formation and the morphology diagram of possible structures in two-dimensional diffusional growth. *Phys Rev E* 54(3):2714–2722. <https://doi.org/10.1103/physreve.54.2714>
47. Lim KKK, Ishak ZAM, Ishiaku US, Fuad AMY, Yusof AH, Czigan T, Pukanszky B, Ogunniyi DS (2005) High-density polyethylene/ultrahigh-molecular-weight polyethylene blend. I. The processing, thermal, and mechanical properties. *J Appl Polym Sci* 97(1):413–425
48. Jariyavidyanont K, Williams JL, Rhoades AM, Kühnert I, Focke W, Androsch R (2018) Crystallization of polyamide 11 during injection molding. *Polym Eng Sci* 58(7):1053–1061. <https://doi.org/10.1002/pen.24665>
49. Kong W, Zhu B, Su F, Wang Z, Shao C, Wang Y, Liu C, Shen C (2019) Melting temperature, concentration and cooling rate-dependent nucleating ability of a self-assembly aryl amide nucleator on poly(lactic acid) crystallization. *Polymer* 168:77–85. <https://doi.org/10.1016/j.polymer.2019.02.019>

Publisher's Note Springer Nature remains neutral with regard to jurisdictional claims in published maps and institutional affiliations.